Signatures of star formation around Sgr A*: an update

Tomas James & Serena Viti

February 14, 2020

Preamble

The project's primary objective is as follows: to take SiO and SO observations around Sgr A* and attempt to reproduce their fluxes using protostellar outflow driven shock models and radiative transfer.

Given the scope of this problem - and its associated computational complexity - we've begun by focusing on exploring and constraining our parameter space, i.e. given the observations, what broad range of physical parameters are capable of producing such observations? Our objective is to use these findings to inform the next stage of the project where we can explore a data motivated and narrower range of parameters in more detail using complex chemical models.

To do this initial exploration we've utilised a Bayesian inference technique to determine the posterior probability distributions of each of the free parameters in our model, as well as the joint distributions of best fitting parameters.

We've focused on a representative pair of SiO and SO observations here, which was selected as the J1 source in the observation outline document; for convenience it attached to the end of this document.

Parameter ranges

Given the proposition that the data is a direct result of shock activity, we use this to begin constraining the physical parameters in our models before attempting to analytically constrain the ranges further. Our initial ranges are as shown in Table 1.

We define a model as being a collection of parameters

With 4 free parameters (therefore 4-dimensions in any model utilising them) and extensive ranges over orders of magnitude in each dimension, it is crucial to constrain this parameter space even further in order to maximise computational efficiency. To exclude un-physical parameters we utilise a Bayesian inference technique to assess how likely a randomly selected combination

Parameter	**Range**
T (K)	10-1000
n_H (cm^{-3})	10^2-10^7
N_{SiO} (cm^{-2})	10^{11}-10^{18}
N_{SO} (cm^{-2})	10^{11}-10^{18}

Table 1: The pre-constrained parameter spaces explored in this preliminary study.

of parameters is to have produced the series of data points observed. Thus we are permitted to explore the entirety of the parameter ranges defined in Table 1 to constrain our parameter space.

Bayesian inference

Bayesian inference relies on Bayes' theorem which is formally defined, for a given model θ and data d, as:

$$P(\theta|d) = \frac{P(d|\theta)P(\theta)}{P(d)} \tag{1}$$

$P(\theta|d)$ is defined as the probability of the model θ fitting the data d given that the data is correct (known as "the posterior probability"). $P(d|\theta)$ is the probability of having obtained the data d given a particular model θ (known as "the likelihood"). $P(\theta)$ is defined as the probability of the model θ being correct ("the prior") and $P(d)$ is the probability that the data is correct ("the evidence", in this instance a simple scaling factor to ensure the PDF sums to 1). We define the data as being the observed fluxes, whilst the model is the line flux determined from a radiative transfer model with inputs being within the ranges defined in Table 1.

By assuming that the data d is discrete and that the model θ may be continuous, one can construct a "posterior distribution" of how likely a continuous spectrum of models is to fit the discrete data. Key to this assumption, however, are the values (or distributions) assigned to the likelihood $P(d|\theta)$ and prior $P(\theta)$.

As an initial assumption we can state that any model is equally as likely as any other. This results in a "flat prior", i.e. the value of the distribution at each model is the same. The likelihood function is somewhat more complex, though we can express it as:

$$P(d|\theta) = e^{-\frac{1}{2}\chi^2} \tag{2}$$

Where χ^2 represents the Chi-squared statistic, i.e.

$$\chi^2 = \sum_i \frac{(d_i - \theta_i)^2}{\sigma_i^2} \tag{3}$$

Where d_i is the ith value of the data, θ_i is the ith value of the model corresponding to d_i and σ_i is the error associated with d_i.

By exponentiating the goodness-of-fit metric we can construct a probability to serve as our likelihood, where the better the fit the greater the probability (and therefore the more likely).

We may assign confidence intervals to the results determined from this technique by finding the models in the posterior distribution that lie within 1σ and 2σ of the mean.

Methodology

Key to the use of Bayes' theorem is the principle of θ being a random variable. We therefore have to randomly select generated values of the parameters that constitute our model: we select gas temperature, gas density, SiO column density and SO column density from underlying uniform distribution for each of these parameters; these are our 4 free parameters.

We then verify that these values fall within the pre-constrained and acceptable range in Table 1: This then forms our prior. An exact value of the prior is not necessary at this stage, as $P(d)$ is used to normalise the posterior (as discussed earlier).

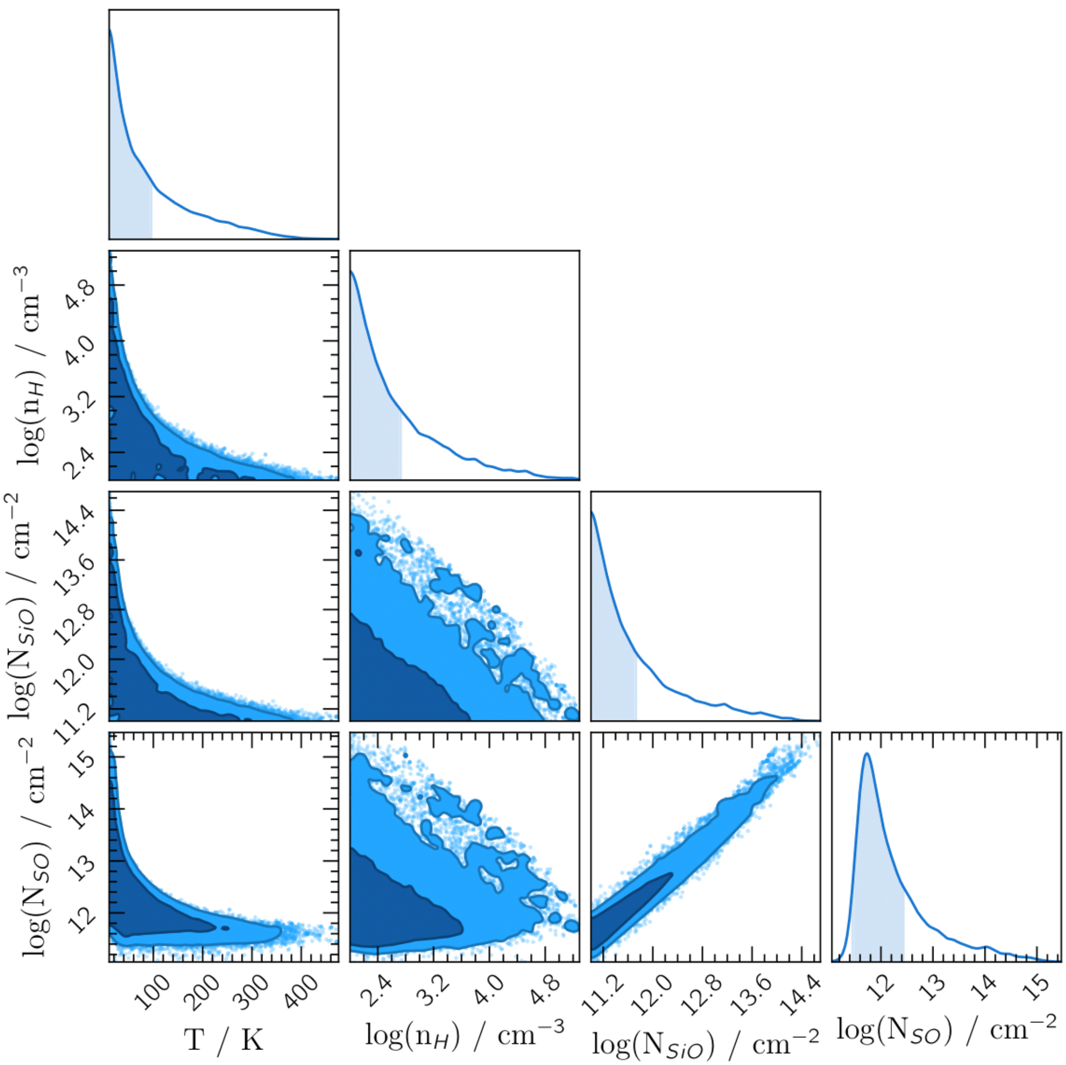

Figure 1: The posterior and joint distributions for the J1 source.

We then run a radiative transfer model using Radex (https://home.strw.leidenuniv.nl/ moldata/radex.html) for the selected parameters to determine the line flux of the relevant transition: 7-6 in SiO and 8(7) - 7(6) in SO. Subsequently using the inference technique described earlier and repeating this process (so as to sample the entire parameter range) 1×10^5 instances produces Figure 1.

Results

The subplots along the hypotenuse of this plot are the posterior distributions, and the 6 other subplots represent 2D joint distributions of the best fitting parameters for the J1 source. The shaded regions in the posterior sub-plots indicates everything within 1σ of the mean, which corresponds to the dark blue regions in the joint distributions. The light blue regions in the joint distributions represents everything within 1σ of the mean.

A clear degeneracy between temperature and the other 3 parameters is observed in the first column of the plot. Interestingly the temperature range capable of producing fluxes that are commensurate with the J1 fluxes is between $10 - 400$ K. In turn, we find that the valid density range is $10^2 - 10^5$ cm^{-3}. In terms of SiO and SO column densities this represents validity ranges of $10^{11} - 10^{14}$ in SiO and $10^{12} - 10^{15}$ in SO.

The first subplot in the third column shows how the column densities of both SiO and SO vary with one another. Interestingly here we see a clear linear relationship between the two, though further investigation across further sources - not just the J1 source - is required ti pinpoint the exact nature of this relationship. Speculatively this could be the result of physical shock action evaporating both Si and SO from the grains, where the evaporated Si reacts with gas-phase O to produce SiO. There is no evidence, at this preliminary stage, of a chemical relationship between SiO and SO.

Also of interest is the posterior distributions tending to lower values of their respective parameters. Considering, however, that this technique relies on 2 points in 1 source we are cautious that this tendency could represent a specific feature of the J1 source and not a global trend across the rest of the observed sources.

Next steps

Our next steps are to as follows:

- Run this technique across each source in the observation to build up maps of the likely parameters as a function of spatial position on the sky
- Use the likely parameter ranges from this study as inputs to a chemical shock model to build up chemical abundance information as a function of time for representative shocks
- Select snapshots of the abundances at specific time instances through the shock and feed in to Radex to construct flux information
- Subsequently compare the Radex fluxes with the data for each source to match likely initial shock parameters to each source on the sky

Source	α (J2000) 17^h45^m	δ (J2000) $-29^\circ 00'$	Sample (beam)	Emission Line	T_L (mJy)	v (km s^{-1})	Δv (km s^{-1})	I_{SiO}/I_{SO}
N3	40.62	24.05	1.00	SiO 7–6	58.6 ± 3.6	-25.56	27.6	
IRS7	40.04	22.76	1.00	SO 8(7)–7(6)	16.3 ± 3.1	32.80	20.9	
N8	40.85	12.88	1.00	SiO 7–6	21.29 ± 9.9	39.52	11.8	0.44 ± 0.22
				SO 8(7)–7(6)	38.3 ± 7.7	38.73	15.0	
N7a	40.88	12.23	10.65	SiO 7–6	8.40 ± 0.92	41.23	13.9	0.48 ± 0.06
				SO 8(7)–7(6)	14.9 ± 0.78	40.16	16.2	
N7b	41.04	13.24	19.59	SiO 7–6	7.22 ± 0.43	39.33	13.9	0.60 ± 0.04
				SO 8(7)–7(6)	10.8 ± 0.39	41.12	15.5	
				CH_3OH_2 2(1,1)–2(0,2)	5.5 ± 0.70	37.68	8.68	

Source	α (J2000) 17^h45^m	δ (J2000) $-29°00'$	Sample (beam)	Emission Line	T_L (mJy)	v (km s^{-1})	Δv (km s^{-1})	I_{SiO}/I_{SO}
G1	43.92	28.07	14.8	SiO 7–6	5.84 ± 0.42	67.47	35.4	0.88 ± 0.08
				SO 8(7)–7(6)	7.77 ± 0.5	64.58	30.3	
				CH_3OH_2 2(1,1)-2(0,2)	4.49 ± 0.47	59.29	31.7	
G2	43.77	16.19	73.6	SiO 7–6	9.53 ± 0.10	56.84	19.7	-0.75 ± -0.01
				SO 8(7)–7(6)	16.7 ± 0.13	55.64	-15.0	
				CH_3OH_2 2(1,1)–2(0,2)	9.57 ± 0.12	56.14	15.6	
				H_2CS 9(1,9)–8(1,8)	6.6 ± 0.19	54.66	9.99	
				OCS 25–24	1.72 ± 0.16	54.34	12.5	
G3a	43.82	25.43	1.59	SiO 7–6	32.2 ± 3.8	53.65	9.86	0.92 ± 0.15
				SO 8(7)–7(6)	39.2 ± 4.3	52.77	8.82	
				CH_3OH_2 2(1,1)–2(0,2)	29.1 ± 3.9	54.01	9.7	
				H_2CS 9(1,9)–8(1,8)	21.2 ± 4.4	53.24	8.42	
G3b	43.87	26.05	2.24	SiO 7–6	35.1 ± 3.5	56.66	10.6	0.68 ± 0.08
				SO 8(7)–7(6)	48.6 ± 3.3	56.98	11.2	
				CH_3OH_2 2(1,1)–2(0,2)	22.5 ± 3.0	57.15	12.2	
				H_2CS 9(1,9)–8(1,8)	16.4 ± 3.7	55.51	10.1	
G4	43.41	24.51	2.85	SiO 7–6	20.3 ± 3.1	52.59	11.2	0.72 ± 0.13
				SO 8(7)–7(6)	25.7 ± 2.8	53.18	12.3	
				CH_3OH_2 2(1,1)–2(0,2)	14.5 ± 2.7	52.37	13.0	
G5	42.32	8.549	11.6	SiO 7–6	39.0 ± 4.7	55.18	15.5	0.93 ± 0.15
				SO 8(7)–7(6)	36.1 ± 4.0	56.19	18.1	
				CH_3OH_2 2(1,1)–2(0,2)	39.9 ± 4.9	54.99	14.9	
				H_2CS 9(1,9)–8(1,8)	17.6 ± 5.3	55.48	13.8	
D1	42.28	47.11	3.69	SiO 7–6	14.5 ± 1.4	107.1	19.6	0.7 ± 0.08
				SO 8(7)–7(6)	33.2 ± 2.2	107.5	12.2	
D2	41.90	47.76	5.52	SiO 7–6	14.4 ± 0.7	106.3	17.3	0.65 ± 0.04
				SO 8(7)–7(6)	25.4 ± 0.8	106.0	15.1	
D3	41.94	49.41	4.2	SiO 7–6	4.61 ± 0.58	109.8	21.3	0.55 ± 0.0.08
					4.51 ± 0.6	75.89	20.5	0.46 ± 0.07
				SO 8(7)–7(6)	11.2 ± 0.77	108.0	15.8	
					9.55 ± 0.59	76.10	21.1	
D4	41.80	47.44	3.3	SiO 7–6	16.3 ± 1.3	107.31	11.7	0.62 ± 0.06
				SO 8(7)–7(6)	23.3 ± 1.2	106.34	13.2	
				CH_3OH_2 2(1,1)–2(0,2)	6.53 ± 1.4	107.233	11.0 &	
D5	41.88	51.00	4.04	SiO 7–6	4.75 ± 0.74	77.92	18.8	0.33 ± 0.05
				SO 8(7)–7(6)	12.1 ± 0.63	76.81	22.1	
D6	41.72	48.78	1.63	SiO 7–6	15.5 ± 3.1	-12.20	9.44	0.71 ± 0.17
				SO 8(7)–7(6)	12.9 ± 1.8	-14.01	15.9	
D7	41.77	44.10	1.65	SiO 7–6	10.9 ± 2.2	93.44	13.3	0.67 ± 0.16
				SO 8(7)–7(6)	19.5 ± 2.6	93.69	11.1	
H1a	39.38	51.18	3.1	SiO 7–6	18.4 ± 1.1	35.10	14.7	0.83 ± 0.07
				SO 8(7)–7(6)	25.6 ± 1.3	34.95	12.7	
				CH_3OH_2 2(1,1)–2(0,2)	4.96 ± 0.88	35.74	19.3	
H1b	39.39	50.36	2.3	SiO 7–6	22.3 ± 1.1	30.53	21.7	1.24 ± 0.1
				SO 8(7)–7(6)	18.2 ± 1.1	30.61	21.4	
				CH_3OH_2 2(1,1)–2(0,2)	6.49 ± 1.3	28.36	17.2	
H2	39.60	51.33	2.6	SiO 7–6	17.5 ± 1.7	37.15	15.6	1.85 ± 0.37
				SO 8(7)–7(6)	12.6 ± 2.2	36.92	11.7	
H3	39.70	51.26	1.1	SiO 7–6	14.2 ± 1.7	53.01	28.2	1.78 ± 0.43
				SO 8(7)–7(6)	10.3 ± 2.2	48.21	21.9	
H4	39.76	46.03	2.11	SiO 7–6	13.5 ± 0.97	73.59	32.9	2.04 ± 0.34
				SO 8(7)–7(6)	7.24 ± 1.1	70.22	30.1	

Source	α (J2000) 17^h45^m	δ (J2000) $-29^\circ 00'$	Sample (beam)	Emission Line	T_L (mJy)	v (km s^{-1})	Δv (km s^{-1})	I_{SiO}/I_{SO}
J1	38.14	1.647	1.3	SiO 7–6	14.3 ± 2.9	62.28	11.3	0.95 ± 0.27
				SO 8(7)–7(6)	18.5 ± 3.6	60.90	9.23	
				CH_3OH_2 2(1,1)–2(0,2)	8.42 ± 2.4	60.49	13.7	
				H_2CS 9(1,9)–8(1,8)	6.57 ± 1.9	60.76	17.5	
J2	38.15	0.01	2.2	SiO 7–6	46.9 ± 1.0	67.16	27.5	2.26 ± 0.12
				SO 8(7)–7(6)	25.0 ± 1.2	65.70	22.8	
J3	38.10	2.82	5.2	SiO 7–6	14.6 ± 0.81	75.19	14.3	0.67 ± 0.04
				SO 8(7)–7(6)	25.5 ± 0.94	74.50	12.3	
				CH_3OH_2 2(1,1)–2(0,2)	10.2 ± 0.87	73.31	13.3	
				H_2CS 9(1,9)–8(1,8)	6.13 ± 1.6	75.00	7.43	
J4	38.25	59.44	2.06	SiO 7–6	10.3 ± 2.2	68.63	12.7	0.88 ± 0.25
				SO 8(7)–7(6)	14.6 ± 2.8	68.91	10.2	
				CH_3OH_2 2(1,1)–2(0,2)	10.8 ± 4.4	67.94	6.46	
K1	38.34	38.38	2.61	SiO 7–6	16.6 ± 1.8	-5.85	12.6	0.67 ± 0.09
				SO 8(7)–7(6)	21.6 ± 1.6	-6.27	14.4	
K2	38.23	40.30	3.03	SiO 7–6	17.5 ± 2.1	-9.06	10.3	0.71 ± 0.1
				SO 8(7)–7(6)	21.4 ± 1.8	-7.60	11.9	
K3	38.26	41.39	1.83	SiO 7–6	11.4 ± 1.8	4.86	14.9	0.55 ± 0.1
				SO 8(7)–7(6)	18.7 ± 1.7	2.45	16.5	
K4	38.40	42.32	3.35	SiO 7–6	14.6 ± 1.2	-17.53	13.9	0.65 ± 0.06
				SO 8(7)–7(6)	22.7 ± 1.2	-18.35	13.7	
K5a	38.23	42.06	3.35	SiO 7–6	9.71 ± 1.5	-15.30	11.7	0.41 ± 0.07
				SO 8(7)–7(6)	13.7 ± 0.89	-10.31	20.0	
K5b	38.31	42.90	2.94	SiO 7–6	8.55 ± 1.3	-20.32	14.8	0.59 ± 0.11
				SO 8(7)–7(6)	16.3 ± 1.5	-20.30	13.1	
K5c	38.22	42.80	2.11	SiO 7–6	8.55 ± 1.3	-20.32	14.8	0.59 ± 0.11
				SO 8(7)–7(6)	16.3 ± 1.5	-20.30	13.1	
K6a	38.09	42.12	3.63	SiO 7–6	11.6 ± 1.1	-1.67	20.7	0.62 ± 0.07
				SO 8(7)–7(6)	19.4 ± 1.1	-3.04	20.1	
K6b	38.01	42.17	2.44	SiO 7–6	10.3 ± 1.6	-13.41	19.8	0.58 ± 0.1
				SO 8(7)–7(6)	19.0 ± 1.7	-12.71	18.6	
K7a	38.12	44.66	7.20	SiO 7–6	21.4 ± 1.1	-42.07	13.7	0.61 ± 0.04
				SO 8(7)–7(6)	35.5 ± 1.1	-41.93	13.5	
				CH_3OH_2 2(1,1)–2(0,2)	4.99 ± 0.94	-39.19	15.4	
K7b	38.09	45.52	2.50	SiO 7–6	12.3 ± 3.0	-50.34	15.3	0.7 ± 0.21
				SO 8(7)–7(6)	18.3 ± 3.2	-45.76	14.7	
K8a	37.98	47.01	5.00	SiO 7–6	25.6 ± 1.5	-43.72	25.9	0.69 ± 0.05
				SO 8(7)–7(6)	41.9 ± 1.7	-44.99	23.0	
K8b	38.02	47.97	6.10	SiO 7–6	23.9 ± 1.7	-40.48	21.9	1.90 ± 0.33
					13.1 ± 2.1	-10.80	17.8	0.61 ± 0.11
				SO 8(7)–7(6)	13.1 ± 2.1	-41.07	21.0	
					23.7 ± 2.3	-9.99	16.2	
K9	38.41	45.39	1.83	SiO 7–6	12.4 ± 1.6	-3.19	26.6	0.55 ± 0.08
				SO 8(7)–7(6)	24.6 ± 1.7	-5.23	24.4	
K10	38.48	46.14	2.94	SiO 7–6	13.0 ± 1.6	-24.71	21.0	0.8 ± 0.13
				SO 8(7)–7(6)	18.5 ± 1.8	-23.93	18.4	
K11	38.51	47.07	1.13	SiO 7–6	11.8 ± 3.7	-16.19	22.7	0.59 ± 0.22
				SO 8(7)–7(6)	23.8 ± 4.4	-20.11	19.0	
K12	38.56	47.52	1.58	SiO 7–6	13.5 ± 5.2	-28.22	15.4	0.48 ± 0.2
				SO 8(7)–7(6)	29.1 ± 5.3	-28.69	15.0	

Source	α (J2000) 17^h45^m	δ (J2000) $-29^\circ00'$	Sample (beam)	Emission Line	T_L (mJy)	v (km s^{-1})	Δv (km s^{-1})	I_{SiO}/I_{SO}
K13a	38.60	48.68	5.85	SiO 7–6	16.3 ± 2.7	-92.39	14.5	1.49 ± 0.78
				SO 8(7)–7(6)	11.1 ± 5.5	-95.18	14.3	
				OCS 25–24	11.1 ± 5.5	-92.99	7.15	
K13b	38.58	49.50	2.09	SiO 7–6	18.0 ± 7.4	-83.93	16.4	0.51 ± 0.23
				SO 8(7)–7(6)	41.4 ± 8.6	-83.68	14.0	
K14	38.42	46.46	1.81	SiO 7–6	13.9 ± 3.8	-26.31	14.1	0.73 ± 0.25
				SO 8(7)–7(6)	17.5 ± 3.5	-23.83	15.3	
K15a	38.29	46.18	4.50	SiO 7–6	19.5 ± 2.3	-9.54	9.75	1.01 ± 0.17
				SO 8(7)–7(6)	17.7 ± 2.1	-8.82	10.6	
K15b	38.30	47.27	2.85	SiO 7–6	15.7 ± 3.3	2.05	13.7	0.71 ± 0.18
				SO 8(7)–7(6)	22.7 ± 3.4	1.17	13.3	
K16	38.26	49.87	4.15	SiO 7–6	18.3 ± 5.4	-36.22	10.5	0.5 ± 0.17
				SO 8(7)–7(6)	31.5 ± 4.7	-35.98	12.2	
K17	37.95	50.36	2.94	SiO 7–6	29.2 ± 8.3	-36.32	16.2	1.05 ± 0.43
				SO 8(7)–7(6)	26.9 ± 8.0	-37.58	16.8	
K18	38.81	40.52	7.51	SiO 7–6	6.05 ± 1.1	-14.92	14.7	0.6 ± 0.13
				SO 8(7)–7(6)	9.54 ± 1.0	-16.35	15.6	
K19	38.70	38.51	4.37	SiO 7–6	7.46 ± 0.73	-29.25	29.4	0.91 ± 0.12
				SO 8(7)–7(6)	8.54 ± 0.76	-27.55	28.2	
K20	38.58	31.29	9.93	SiO 7–6	10.3 ± 1.3	-2.82	19.7	0.53 ± 0.08
				SO 8(7)–7(6)	16.0 ± 1.1	-5.92	24.0	
K21a	38.15	32.82	2.03	SiO 7–6	17.5 ± 2.3	32.31	27.1	0.74 ± 0.12
				SO 8(7)–7(6)	25.1 ± 2.4	31.28	25.4	
K21b	38.13	32.09	2.33	SiO 7–6	18.4 ± 4.2	22.53	13.1	0.69 ± 0.19
				SO 8(7)–7(6)	28.6 ± 4.4	21.08	12.3	
K22	37.85	31.02	3.83	SiO 7–6	13.4 ± 5.7	-8.65	14.5	0.66 ± 0.34
				SO 8(7)–7(6)	18.7 ± 5.3	-9.83	15.7	
K23	37.99	35.57	5.45	SiO 7–6	6.86 ± 1.8	51.19	10.4	0.47 ± 0.14
				SO 8(7)–7(6)	15.0 ± 1.8	51.66	10.1	
K24	37.97	36.19	2.49	SiO 7–6	9.11 ± 2.2	-17.10	15.2	0.79 ± 0.24
				SO 8(7)–7(6)	12.6 ± 2.4	-16.90	13.9	

Source	α (J2000) 17^h45^m	δ (J2000) $-29^\circ00'$	Sample (beam)	Emission Line	T_L (mJy)	v (km s^{-1})	Δv (km s^{-1})	I_{SiO}/I_{SO}
L1	39.60	04.29	3.67	SiO 7–6	16.1 ± 1.1	-58.68	20.8	0.81 ± 0.07
				SO 8(7)–7(6)	29.1 ± 1.6	-58.91	14.2	
L2	39.74	05.41	2.25	SiO 7–6	17.2 ± 2.0	-35.33	16.8	0.58 ± 0.08
				SO 8(7)–7(6)	31.7 ± 2.2	-35.60	15.8	
L3	39.79	5.57	1.02	SiO 7–6	7.95 ± 3.3	-62.66	15.6	0.37 ± 0.16
				SO 8(7)–7(6)	22.4 ± 3.4	-61.95	15.1	
L4	38.80	06.84	2.18	SiO 7–6	10.3 ± 1.2	-48.40	23.1	0.47 ± 0.06
				SO 8(7)–7(6)	28.2 ± 1.6	-51.13	18.0	
L5	39.66	06.15	1.99	SiO 7–6	16.7 ± 2.1	-49.29	17.2	0.53 ± 0.08
				SO 8(7)–7(6)	22.4 ± 1.5	-51.23	24.0	
L6	39.70	07.10	5.11	SiO 7–6	13.0 ± 0.71	-55.02	24.5	0.6 ± 0.04
				SO 8(7)–7(6)	26.6 ± 0.87	-54.88	20.0	
L7	39.75	07.79	3.20	SiO 7–6	18.9 ± 1.7	-61.44	17.9	0.43 ± 0.04
				SO 8(7)–7(6)	51.2 ± 1.9	-62.67	15.5	
L8	39.68	07.93	6.58	SiO 7–6	10.1 ± 0.99	-63.48	17.4	0.4 ± 0.04
				SO 8(7)–7(6)	34.2 ± 1.3	-64.93	13.0	
L9	39.81	7.82	2.25	SiO 7–6	6.18 ± 1.6	-57.91	17.5	0.25 ± 0.07
				SO 8(7)–7(6)	28.4 ± 1.8	-60.78	15.3	
L10a	39.81	8.68	2.20	SiO 7–6	12.1 ± 2.4	-60.44	15.2	0.34 ± 0.07
				SO 8(7)–7(6)	28.9 ± 1.9	-59.95	18.6	
L10b	39.78	08.75	2.80	SiO 7–6	14.6 ± 1.6	-64.80	21.1	0.46 ± 0.06
				SO 8(7)–7(6)	39.1 ± 2.0	-64.58	17.2	
L11	30.80	09.66	3.50	SiO 7–6	8.47 ± 3.8	-64.30	7.15	0.2 ± 0.09
				SO 8(7)–7(6)	17.3 ± 1.5	-69.77	17.7	
L12	39.88	9.93	1.78	SiO 7–6	7.32 ± 2.3	-34.75	19.8	0.59 ± 0.22
				SO 8(7)–7(6)	15.0 ± 2.8	-35.23	16.3	
L13	39.88	4.67	5.74	SiO 7–6	7.62 ± 0.31	-46.78	36.6	0.51 ± 0.02
				SO 8(7)–7(6)	18.1 ± 0.38	-46.09	30.0	
L14	39.91	4.06	4.39	SiO 7–6	10.1 ± 0.59	-58.36	24.2	0.62 ± 0.04
				SO 8(7)–7(6)	15.5 ± 0.55	-55.07	25.6	
L15	39.96	3.62	1.78	SiO 7–6	18.2 ± 2.3	-59.76	14.5	0.48 ± 0.07
				SO 8(7)–7(6)	30.8 ± 1.9	-58.14	17.7	
L16	40.00	3.38	1.70	SiO 7–6	10.3 ± 1.4	-52.46	22.9	0.5 ± 0.08
				SO 8(7)–7(6)	26.9 ± 1.8	-51.29	17.5	
L17	40.05	2.33	4.53	SiO 7–6	30.9 ± 0.99	-65.43	18.2	0.74 ± 0.03
				SO 8(7)–7(6)	35.1 ± 0.83	-64.85	21.6	
L18	40.09	2.60	2.97	SiO 7–6	14.1 ± 0.86	-49.59	23.6	0.59 ± 0.04
				SO 8(7)–7(6)	25.9 ± 0.92	-49.22	21.9	
L19	40.12	1.78	4.07	SiO 7–6	9.37 ± 1.3	-45.00	13.8	0.47 ± 0.07
					28.3 ± 0.92	-69.00	20.2	0.80 ± 0.03
				SO 8(7)–7(6)	18.0 ± 1.2	-46.16	15.2	
					35.8 ± 0.92	-68.97	20.0	
L20	40.14	1.13	2.73	SiO 7–6	24.5 ± 1.3	-48.49	20.2	0.65 ± 0.04
				SO 8(7)–7(6)	48.4 ± 1.7	-48.64	15.8	

Source	α (J2000) 17^h45^m	δ (J2000) $-29°00'$	Sample (beam)	Emission Line	T_L (mJy)	v (km s^{-1})	Δv (km s^{-1})	I_{SiO}/I_{SO}
L21	40.15	00.44	3.22	SiO 7–6	16.9 ± 1.2	-51.05	17.8	0.47 ± 0.04
				SO 8(7)–7(6)	31.4 ± 1.1	-52.57	20.4	
L22	40.181	00.89	2.52	SiO 7–6	26.4 ± 1.4	-47.16	19.5	0.54 ± 0.03
				SO 8(7)–7(6)	44.5 ± 1.3	-47.60	21.3	
L23	40.19	1.47	2.88	SiO 7–6	15.2 ± 0.94	-48.15	29.4	0.52 ± 0.04
				SO 8(7)–7(6)	32.6 ± 1.1	-48.62	26.2	
L24	40.25	00.94	4.02	SiO 7–6	17.1 ± 1.1	-62.84	22.1	0.46 ± 0.03
				SO 8(7)–7(6)	37.1 ± 1.1	-62.44	22.0	
L25	40.20	00.14	2.94	SiO 7–6	17.5 ± 0.92	-61.57	29.6	0.66 ± 0.04
				SO 8(7)–7(6)	28.7 ± 1.0	-58.58	27.2	
L26	40.27	59.59	3.35	SiO 7–6	12.4 ± 1.2	-52.84	22.7	0.53 ± 0.06
				SO 8(7)–7(6)	22.6 ± 1.2	-51.51	23.3	
L27	40.28	58.81	1.69	SiO 7–6	17.7 ± 2.8	-30.47	18.8	0.56 ± 0.1
				SO 8(7)–7(6)	26.5 ± 2.3	-29.15	22.6	
L28	40.46	59.67	89.40	SiO 7–6	12.7 ± 0.84	-60.86	19.5	0.62 ± 0.05
				SO 8(7)–7(6)	18.7 ± 0.77	-59.57	21.2	
L29	40.19	3.83	3.09	SiO 7–6	7.54 ± 0.99	-49.50	21.6	0.55 ± 0.08
				SO 8(7)–7(6)	12.2 ± 0.88	-53.33	24.2	
L30	40.47	8.10	3.52	SiO 7–6	14.0 ± 3.1	-26.48	14.9	0.89 ± 0.21
					6.18 ± 4.2	-52.43	10.9	13.46 ± 9.69
				SO 8(7)–7(6)	21.6 ± 2.0	-30.01	10.9	
					12.7 ± 2.7	-63.94	0.394	
M1	41.31	58.84	4.50	SiO 7–6	8.67 ± 1.0	-45.25	14.4	0.65 ± 0.09
				SO 8(7)–7(6)	13.8 ± 1.1	-44.42	14.0	
M2	41.41	59.93	1.00	SiO 7–6	2.98 ± 0.63	-50.17	18.2	0.38 ± 0.09
				SO 8(7)–7(6)	8.22 ± 0.66	-54.28	17.2	
M3	41.38	58.16	2.02	SiO 7–6	6.39 ± 1.9	-42.64	15.4	0.43 ± 0.14
				SO 8(7)–7(6)	9.23 ± 1.2	-44.63	24.8	
M4	41.23	57.77	2.27	SO 8(7)–7(6)	10.8 ± 3.2	23.10	8.21	
				CH_3OH_2 2(1,1)–2(0,2)	8.19 ± 2.2	21.39	12.0	

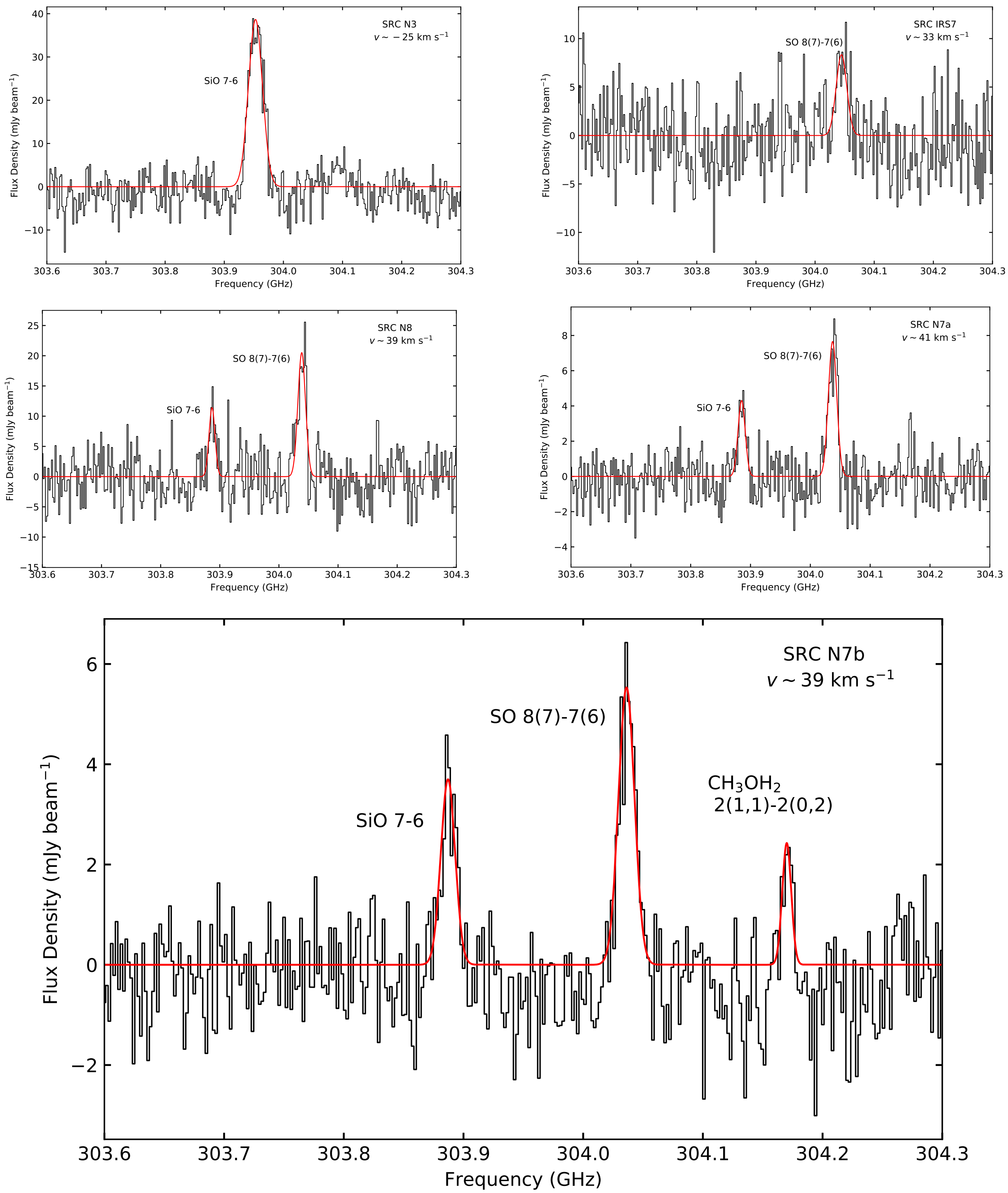
SRC N3
$v \sim -25$ km s^{-1}
SiO 7-6
SRC IRS7
$v \sim 33$ km s^{-1}
SO 8(7)-7(6)
SRC N8
$v \sim 39$ km s^{-1}
SO 8(7)-7(6)
SiO 7-6
SRC N7a
$v \sim 41$ km s^{-1}
SO 8(7)-7(6)
SiO 7-6
SRC N7b
$v \sim 39$ km s^{-1}
SO 8(7)-7(6)
CH_3OH_2
2(1,1)-2(0,2)
SiO 7-6
Flux Density (mJy beam^{-1})
Frequency (GHz)

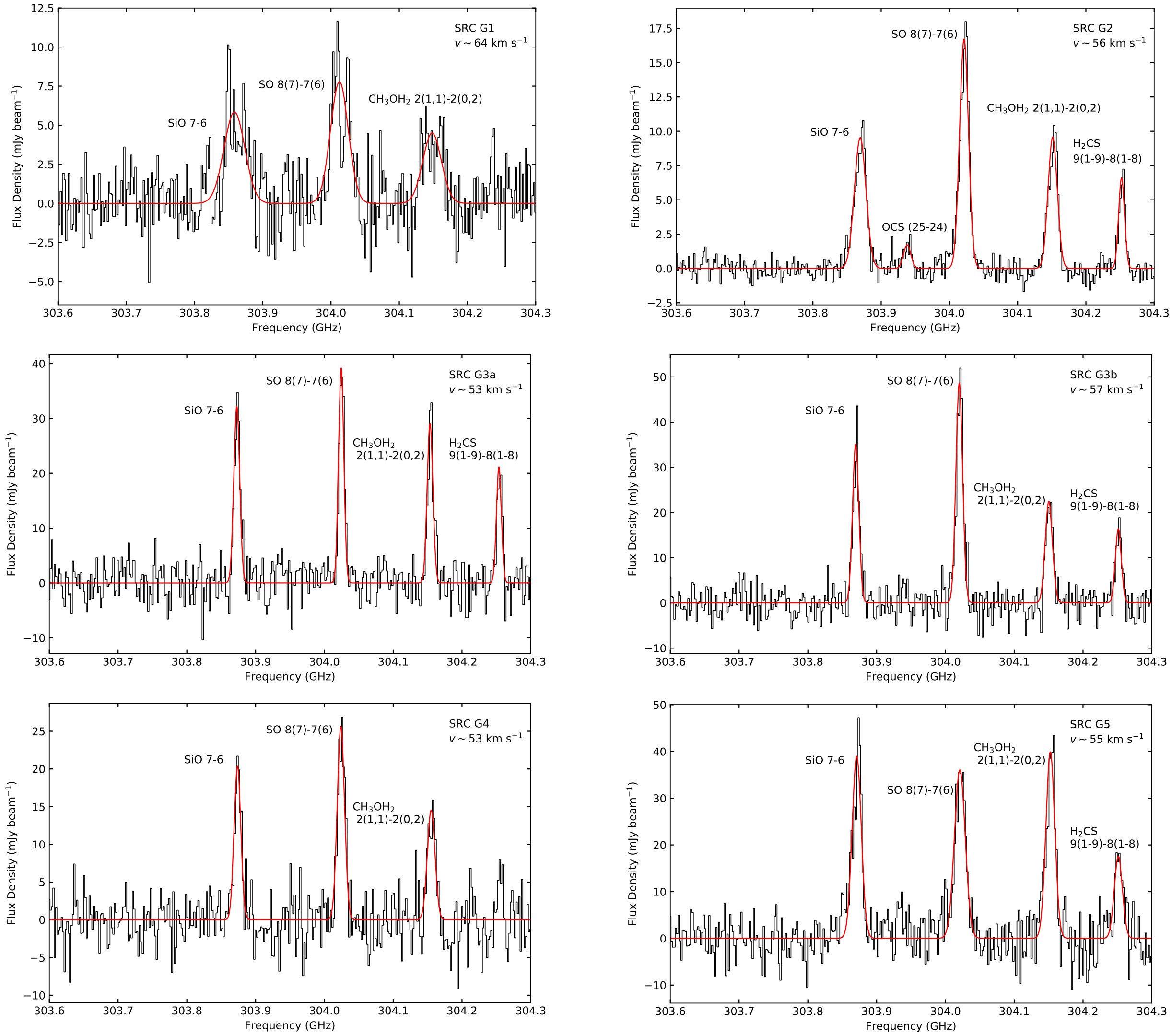
SRC G1
$v \sim 64$ km s^{-1}
SiO 7-6
SO 8(7)-7(6)
CH_3OH_2 2(1,1)-2(0,2)
SRC G2
$v \sim 56$ km s^{-1}
SiO 7-6
OCS (25-24)
SO 8(7)-7(6)
CH_3OH_2 2(1,1)-2(0,2)
H_2CS 9(1-9)-8(1-8)
SRC G3a
$v \sim 53$ km s^{-1}
SRC G3b
$v \sim 57$ km s^{-1}
SRC G4
$v \sim 53$ km s^{-1}
SRC G5
$v \sim 55$ km s^{-1}
Flux Density (mJy beam^{-1})
Frequency (GHz)

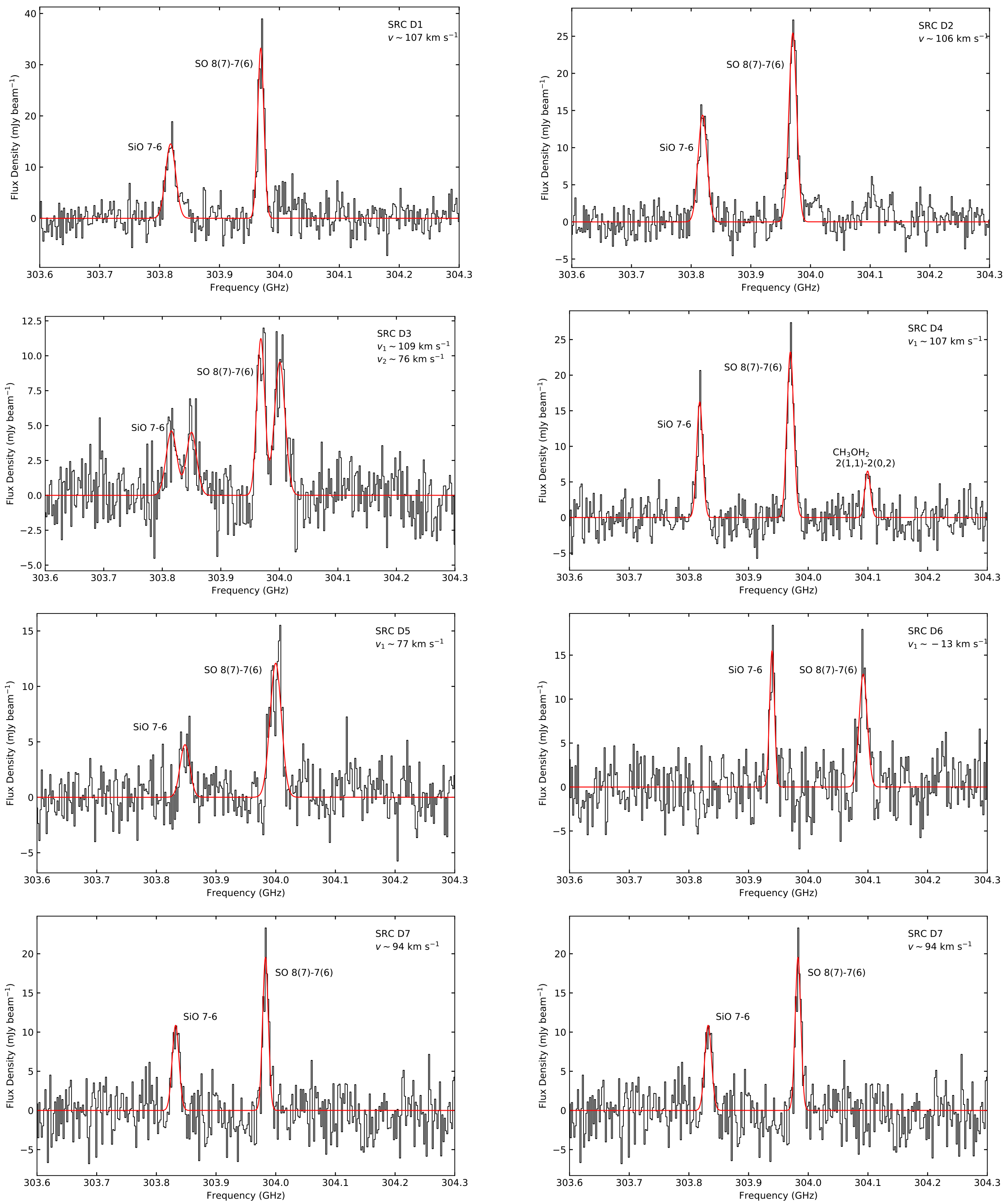
SRC D1
v ~ 107 km s−1
SO 8(7)-7(6)
SiO 7-6
Flux Density (mJy beam−1)
Frequency (GHz)
SRC D2
v ~ 106 km s−1
SO 8(7)-7(6)
SiO 7-6
SRC D3
v1 ~ 109 km s−1
v2 ~ 76 km s−1
SO 8(7)-7(6)
SiO 7-6
SRC D4
v1 ~ 107 km s−1
SO 8(7)-7(6)
SiO 7-6
CH3OH2
2(1,1)-2(0,2)
SRC D5
v1 ~ 77 km s−1
SO 8(7)-7(6)
SiO 7-6
SRC D6
v1 ~ −13 km s−1
SiO 7-6
SO 8(7)-7(6)
SRC D7
v ~ 94 km s−1
SO 8(7)-7(6)
SiO 7-6
SRC D7
v ~ 94 km s−1
SO 8(7)-7(6)
SiO 7-6

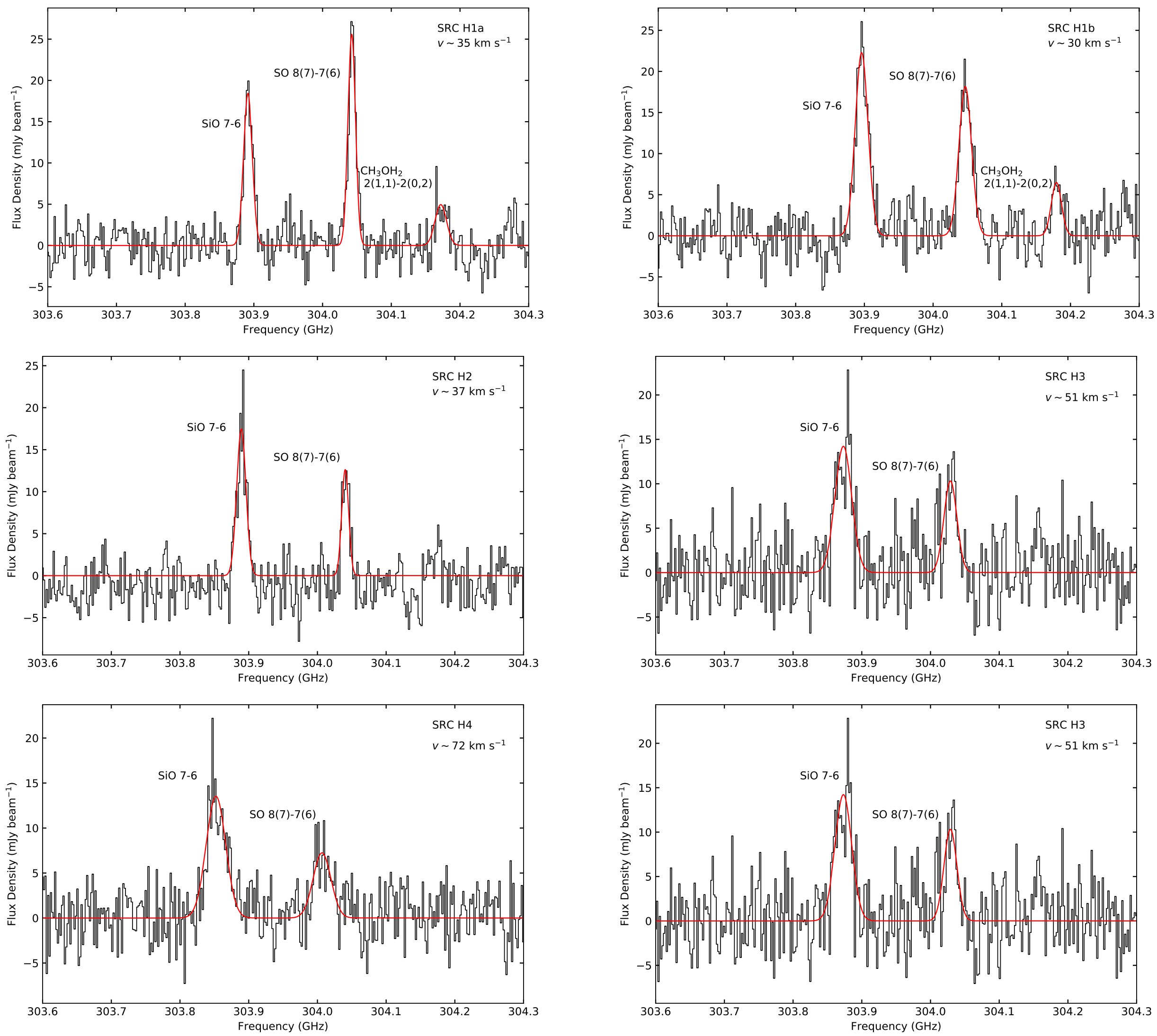
SRC H1a
$v \sim 35$ km s^{-1}
SiO 7-6
SO 8(7)-7(6)
CH_3OH_2
2(1,1)-2(0,2)
SRC H1b
$v \sim 30$ km s^{-1}
SiO 7-6
SO 8(7)-7(6)
CH_3OH_2
2(1,1)-2(0,2)
SRC H2
$v \sim 37$ km s^{-1}
SiO 7-6
SO 8(7)-7(6)
SRC H3
$v \sim 51$ km s^{-1}
SiO 7-6
SO 8(7)-7(6)
SRC H4
$v \sim 72$ km s^{-1}
SiO 7-6
SO 8(7)-7(6)
SRC H3
$v \sim 51$ km s^{-1}
SiO 7-6
SO 8(7)-7(6)
Flux Density (mJy beam^{-1})
Frequency (GHz)

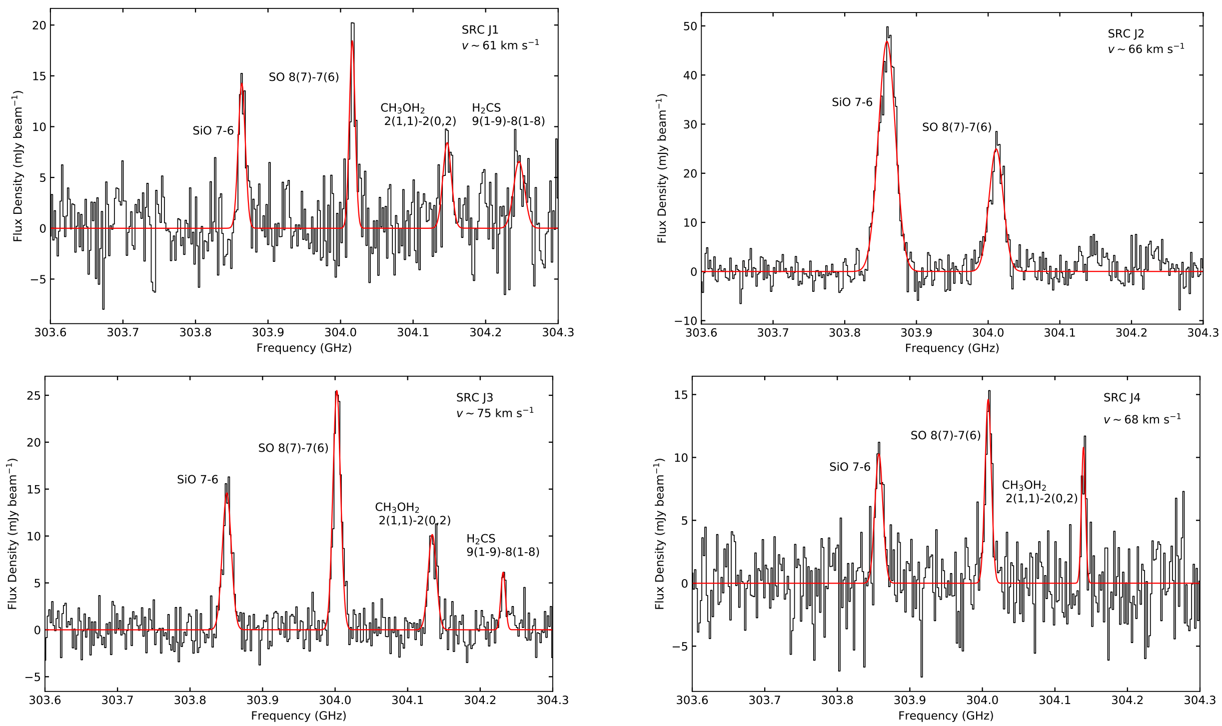
SRC J1
$v \sim 61$ km s^{-1}
SiO 7-6
SO 8(7)-7(6)
CH_3OH_2
2(1,1)-2(0,2)
H_2CS
9(1-9)-8(1-8)
SRC J2
$v \sim 66$ km s^{-1}
SiO 7-6
SO 8(7)-7(6)
SRC J3
$v \sim 75$ km s^{-1}
SiO 7-6
SO 8(7)-7(6)
CH_3OH_2
2(1,1)-2(0,2)
H_2CS
9(1-9)-8(1-8)
SRC J4
$v \sim 68$ km s^{-1}
SiO 7-6
SO 8(7)-7(6)
CH_3OH_2
2(1,1)-2(0,2)
Flux Density (mJy beam^{-1})
Frequency (GHz)

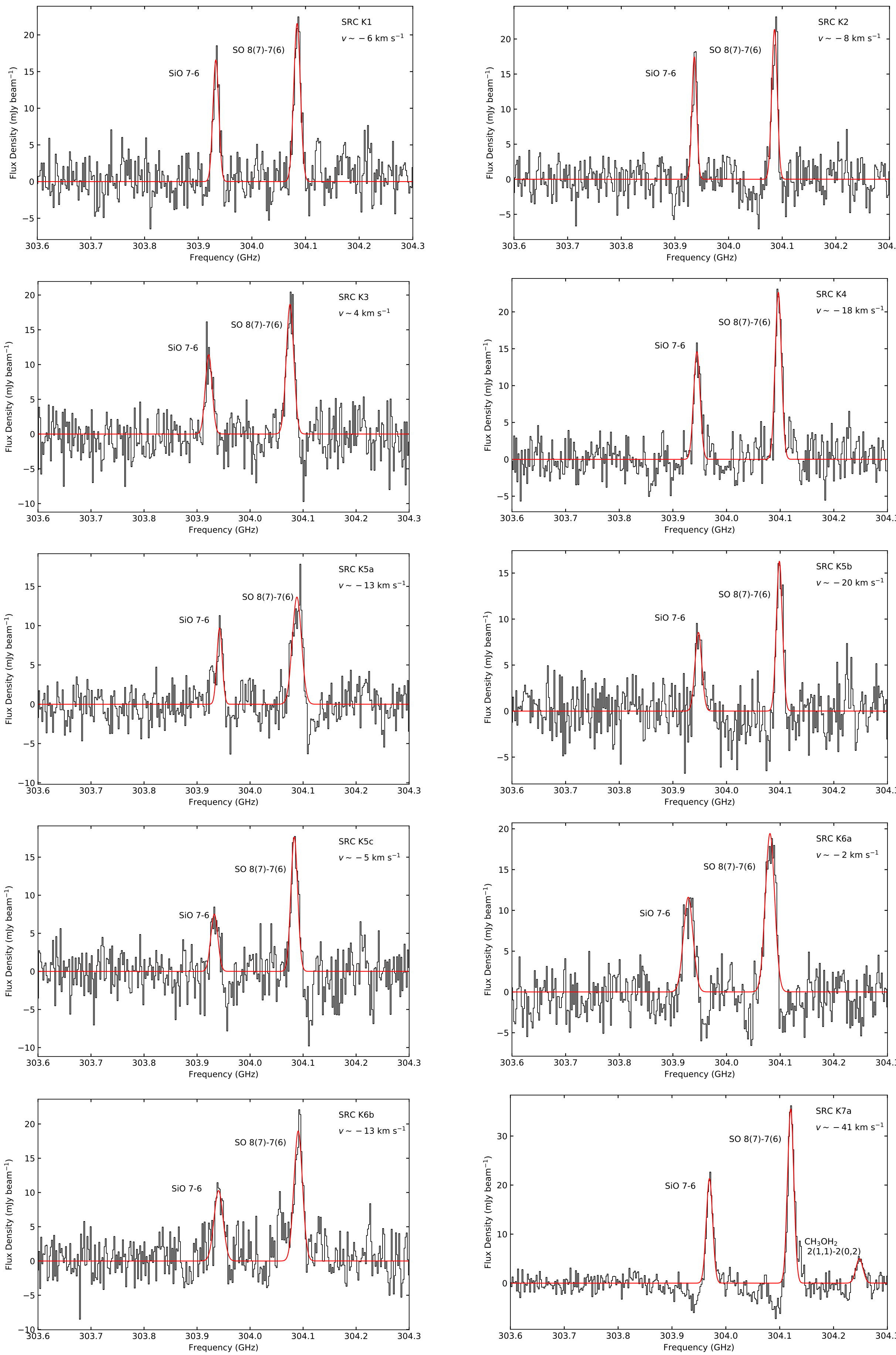
SRC K1
$v \sim -6$ km s^{-1}
SiO 7-6
SO 8(7)-7(6)
SRC K2
$v \sim -8$ km s^{-1}
SiO 7-6
SO 8(7)-7(6)
SRC K3
$v \sim 4$ km s^{-1}
SiO 7-6
SO 8(7)-7(6)
SRC K4
$v \sim -18$ km s^{-1}
SiO 7-6
SO 8(7)-7(6)
SRC K5a
$v \sim -13$ km s^{-1}
SiO 7-6
SO 8(7)-7(6)
SRC K5b
$v \sim -20$ km s^{-1}
SiO 7-6
SO 8(7)-7(6)
SRC K5c
$v \sim -5$ km s^{-1}
SiO 7-6
SO 8(7)-7(6)
SRC K6a
$v \sim -2$ km s^{-1}
SiO 7-6
SO 8(7)-7(6)
SRC K6b
$v \sim -13$ km s^{-1}
SiO 7-6
SO 8(7)-7(6)
SRC K7a
$v \sim -41$ km s^{-1}
SiO 7-6
SO 8(7)-7(6)
CH_3OH_2
2(1,1)-2(0,2)
Flux Density (mJy beam^{-1})
Frequency (GHz)

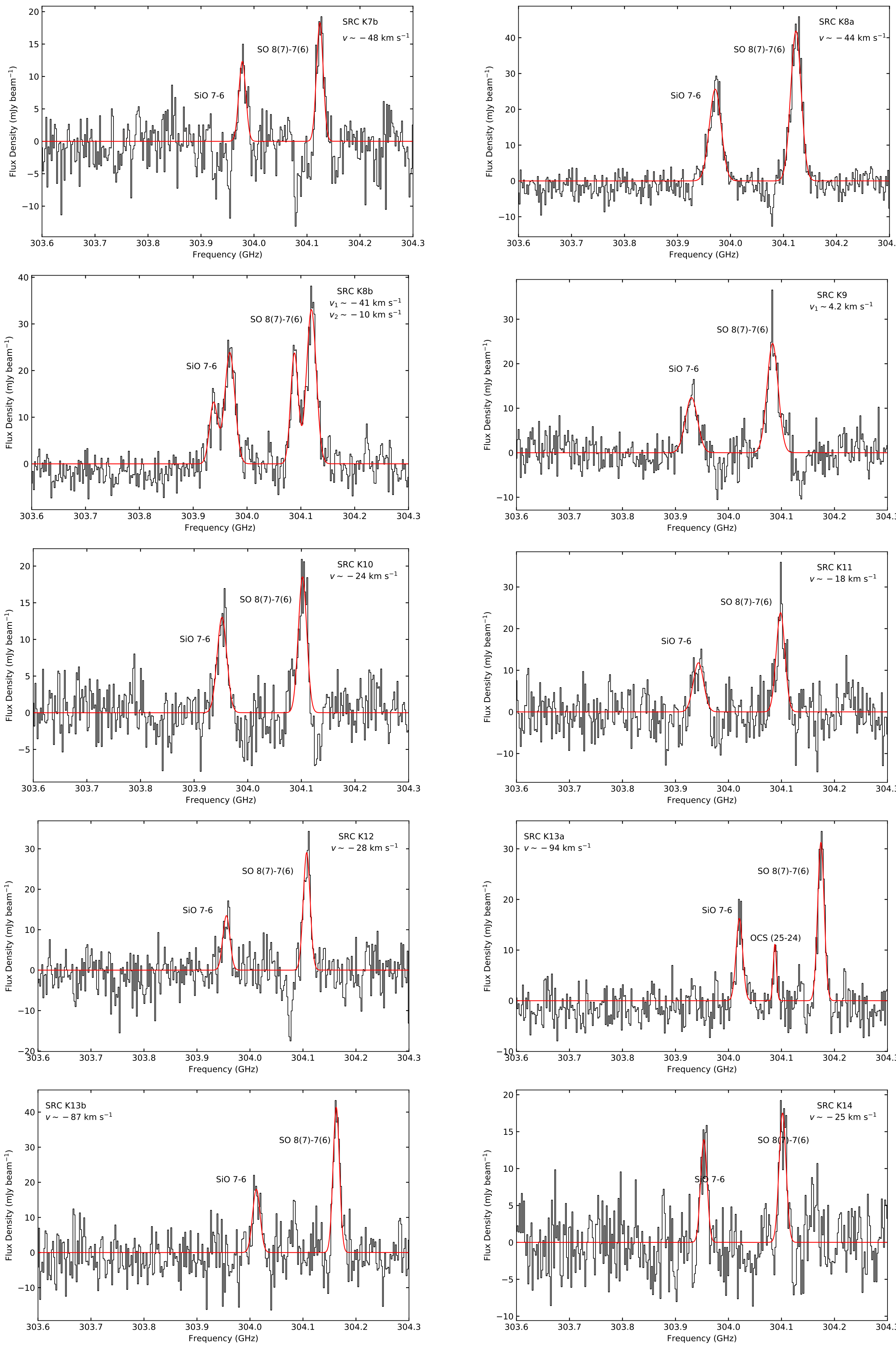
SRC K7b
$v \sim -48$ km s^{-1}
SO 8(7)-7(6)
SiO 7-6
SRC K8a
$v \sim -44$ km s^{-1}
SO 8(7)-7(6)
SiO 7-6
SRC K8b
$v_1 \sim -41$ km s^{-1}
$v_2 \sim -10$ km s^{-1}
SO 8(7)-7(6)
SiO 7-6
SRC K9
$v_1 \sim 4.2$ km s^{-1}
SO 8(7)-7(6)
SiO 7-6
SRC K10
$v \sim -24$ km s^{-1}
SO 8(7)-7(6)
SiO 7-6
SRC K11
$v \sim -18$ km s^{-1}
SO 8(7)-7(6)
SiO 7-6
SRC K12
$v \sim -28$ km s^{-1}
SO 8(7)-7(6)
SiO 7-6
SRC K13a
$v \sim -94$ km s^{-1}
SO 8(7)-7(6)
SiO 7-6
OCS (25-24)
SRC K13b
$v \sim -87$ km s^{-1}
SO 8(7)-7(6)
SiO 7-6
SRC K14
$v \sim -25$ km s^{-1}
SO 8(7)-7(6)
SiO 7-6
Flux Density (mJy beam^{-1})
Frequency (GHz)
303.6
303.7
303.8
303.9
304.0
304.1
304.2
304.3

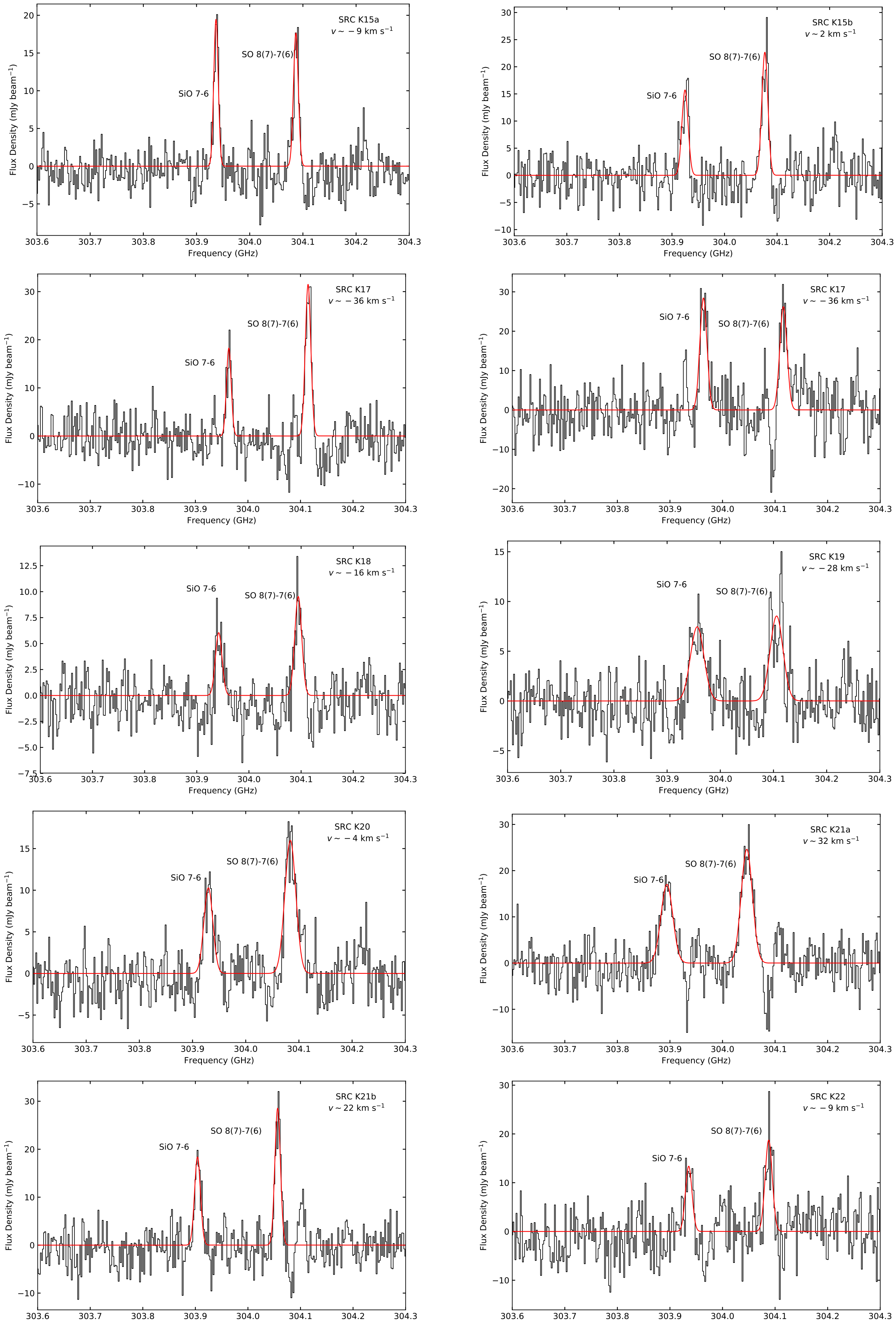
SRC K15a
$v \sim -9$ km s^{-1}
SiO 7-6
SO 8(7)-7(6)
Flux Density (mJy beam^{-1})
Frequency (GHz)
SRC K15b
$v \sim 2$ km s^{-1}
SiO 7-6
SO 8(7)-7(6)
Flux Density (mJy beam^{-1})
Frequency (GHz)
SRC K17
$v \sim -36$ km s^{-1}
SiO 7-6
SO 8(7)-7(6)
Flux Density (mJy beam^{-1})
Frequency (GHz)
SRC K17
$v \sim -36$ km s^{-1}
SiO 7-6
SO 8(7)-7(6)
Flux Density (mJy beam^{-1})
Frequency (GHz)
SRC K18
$v \sim -16$ km s^{-1}
SiO 7-6
SO 8(7)-7(6)
Flux Density (mJy beam^{-1})
Frequency (GHz)
SRC K19
$v \sim -28$ km s^{-1}
SiO 7-6
SO 8(7)-7(6)
Flux Density (mJy beam^{-1})
Frequency (GHz)
SRC K20
$v \sim -4$ km s^{-1}
SiO 7-6
SO 8(7)-7(6)
Flux Density (mJy beam^{-1})
Frequency (GHz)
SRC K21a
$v \sim 32$ km s^{-1}
SiO 7-6
SO 8(7)-7(6)
Flux Density (mJy beam^{-1})
Frequency (GHz)
SRC K21b
$v \sim 22$ km s^{-1}
SiO 7-6
SO 8(7)-7(6)
Flux Density (mJy beam^{-1})
Frequency (GHz)
SRC K22
$v \sim -9$ km s^{-1}
SiO 7-6
SO 8(7)-7(6)
Flux Density (mJy beam^{-1})
Frequency (GHz)

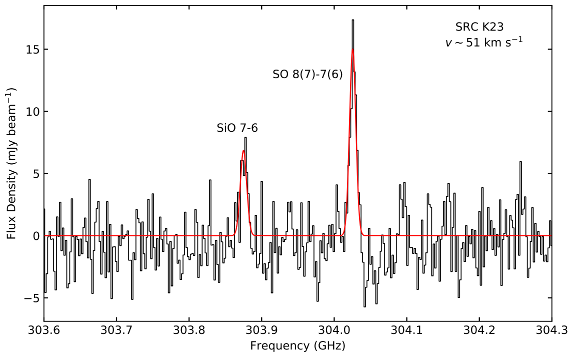
SRC K23
$v \sim 51$ km s^{-1}
SiO 7-6
SO 8(7)-7(6)
Flux Density (mJy beam^{-1})
Frequency (GHz)
303.6
303.7
303.8
303.9
304.0
304.1
304.2
304.3
−5
0
5
10
15

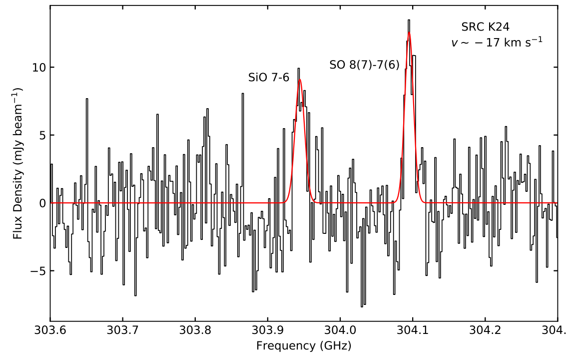
SRC K24
$v \sim -17$ km s^{-1}
SiO 7-6
SO 8(7)-7(6)
Flux Density (mJy beam^{-1})
Frequency (GHz)
303.6
303.7
303.8
303.9
304.0
304.1
304.2
304.3
−5
0
5
10

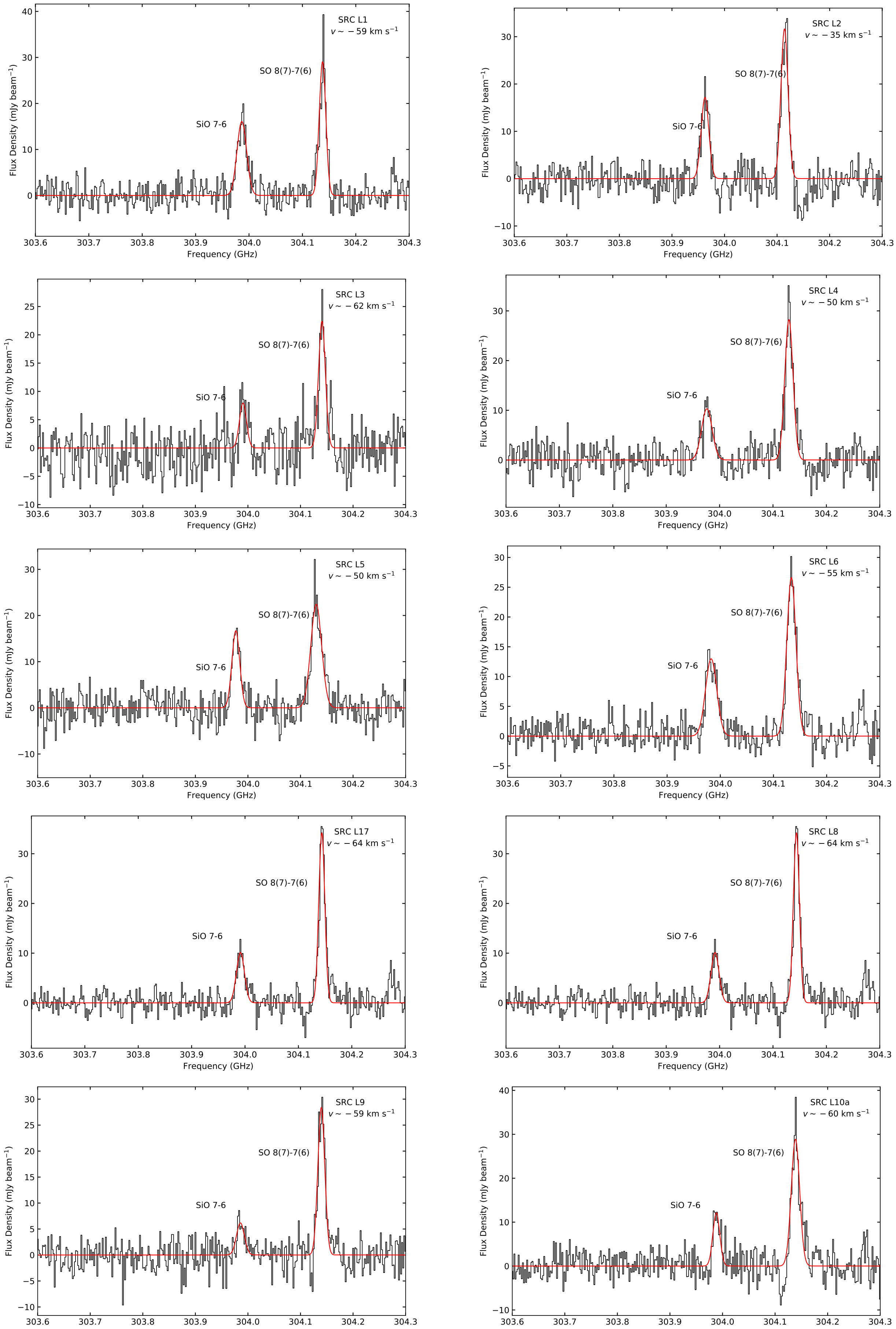
SRC L1
v ∼ −59 km s−1
SO 8(7)-7(6)
SiO 7-6
SRC L2
v ∼ −35 km s−1
SO 8(7)-7(6)
SiO 7-6
SRC L3
v ∼ −62 km s−1
SO 8(7)-7(6)
SiO 7-6
SRC L4
v ∼ −50 km s−1
SO 8(7)-7(6)
SiO 7-6
SRC L5
v ∼ −50 km s−1
SO 8(7)-7(6)
SiO 7-6
SRC L6
v ∼ −55 km s−1
SO 8(7)-7(6)
SiO 7-6
SRC L17
v ∼ −64 km s−1
SO 8(7)-7(6)
SiO 7-6
SRC L8
v ∼ −64 km s−1
SO 8(7)-7(6)
SiO 7-6
SRC L9
v ∼ −59 km s−1
SO 8(7)-7(6)
SiO 7-6
SRC L10a
v ∼ −60 km s−1
SO 8(7)-7(6)
SiO 7-6
Flux Density (mJy beam−1)
Frequency (GHz)

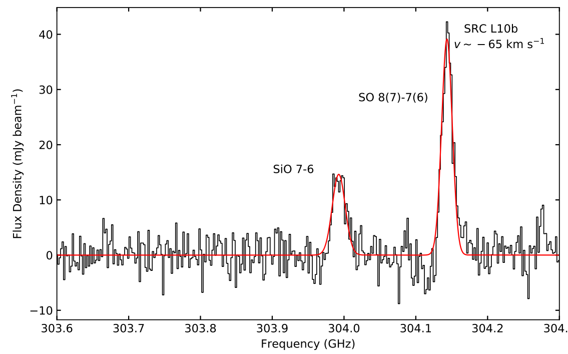
SRC L10b
$v \sim -65$ km s^{-1}
SO 8(7)-7(6)
SiO 7-6
Flux Density (mJy beam^{-1})
Frequency (GHz)

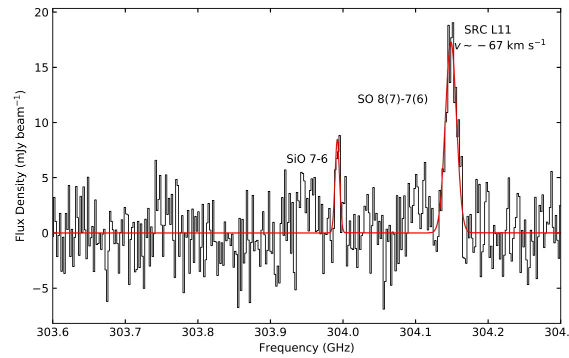
SRC L11
$v \sim -67$ km s^{-1}
SO 8(7)-7(6)
SiO 7-6
Flux Density (mJy beam^{-1})
Frequency (GHz)

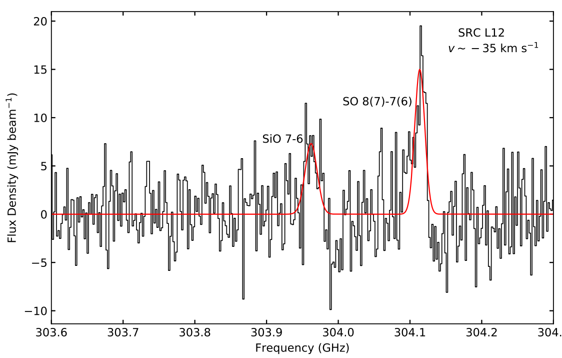
SRC L12
$v \sim -35$ km s^{-1}
SO 8(7)-7(6)
SiO 7-6
Flux Density (mJy beam^{-1})
Frequency (GHz)

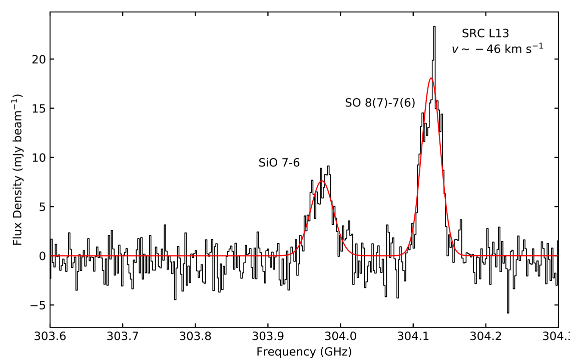
SRC L13
$v \sim -46$ km s^{-1}
SO 8(7)-7(6)
SiO 7-6
Flux Density (mJy beam^{-1})
Frequency (GHz)

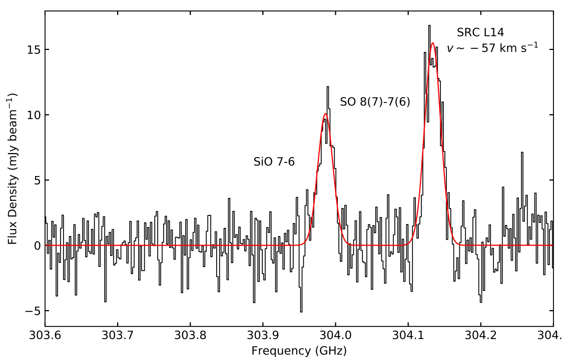
SRC L14
$v \sim -57$ km s^{-1}
SO 8(7)-7(6)
SiO 7-6
Flux Density (mJy beam^{-1})
Frequency (GHz)

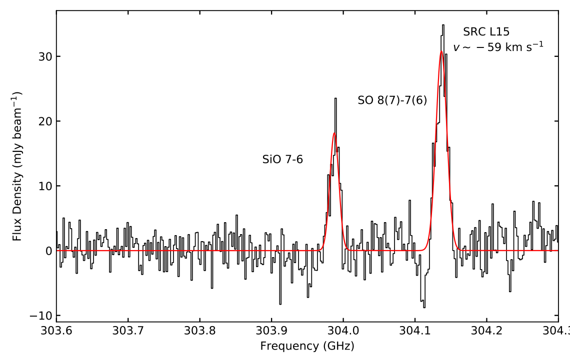
SRC L15
$v \sim -59$ km s^{-1}
SO 8(7)-7(6)
SiO 7-6
Flux Density (mJy beam^{-1})
Frequency (GHz)

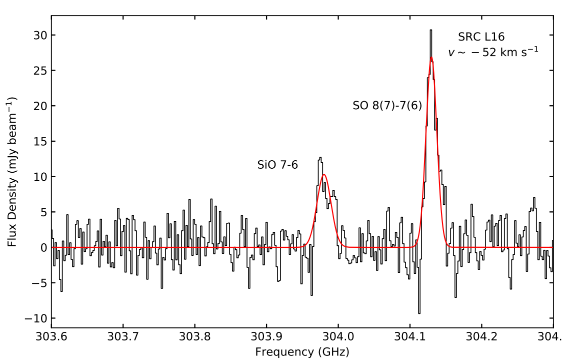
SRC L16
$v \sim -52$ km s^{-1}
SO 8(7)-7(6)
SiO 7-6
Flux Density (mJy beam^{-1})
Frequency (GHz)

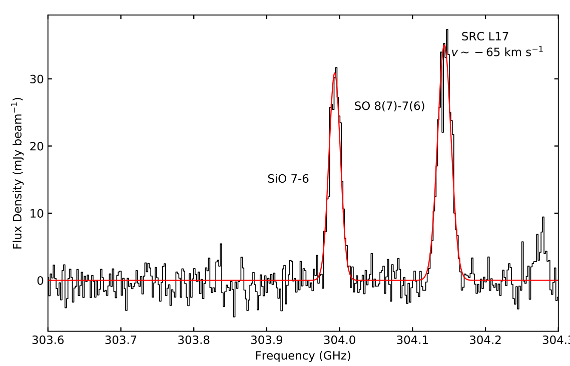
SRC L17
$v \sim -65$ km s^{-1}
SO 8(7)-7(6)
SiO 7-6
Flux Density (mJy beam^{-1})
Frequency (GHz)

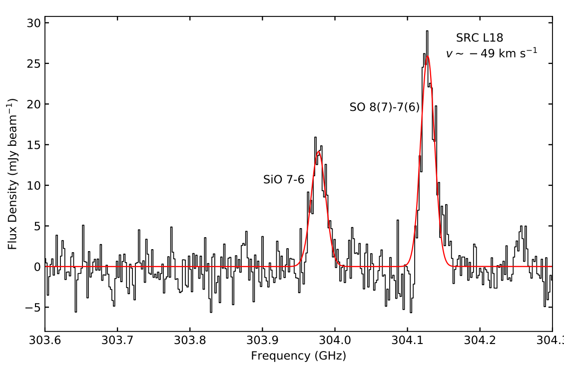
SRC L18
$v \sim -49$ km s^{-1}
SO 8(7)-7(6)
SiO 7-6
Flux Density (mJy beam^{-1})
Frequency (GHz)

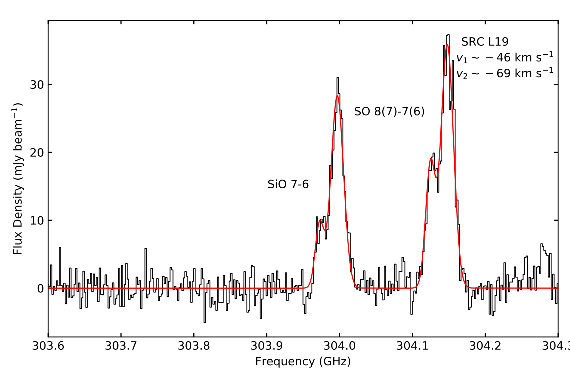
SRC L19
$v_1 \sim -46$ km s^{-1}
$v_2 \sim -69$ km s^{-1}
SO 8(7)-7(6)
SiO 7-6
Flux Density (mJy beam^{-1})
Frequency (GHz)

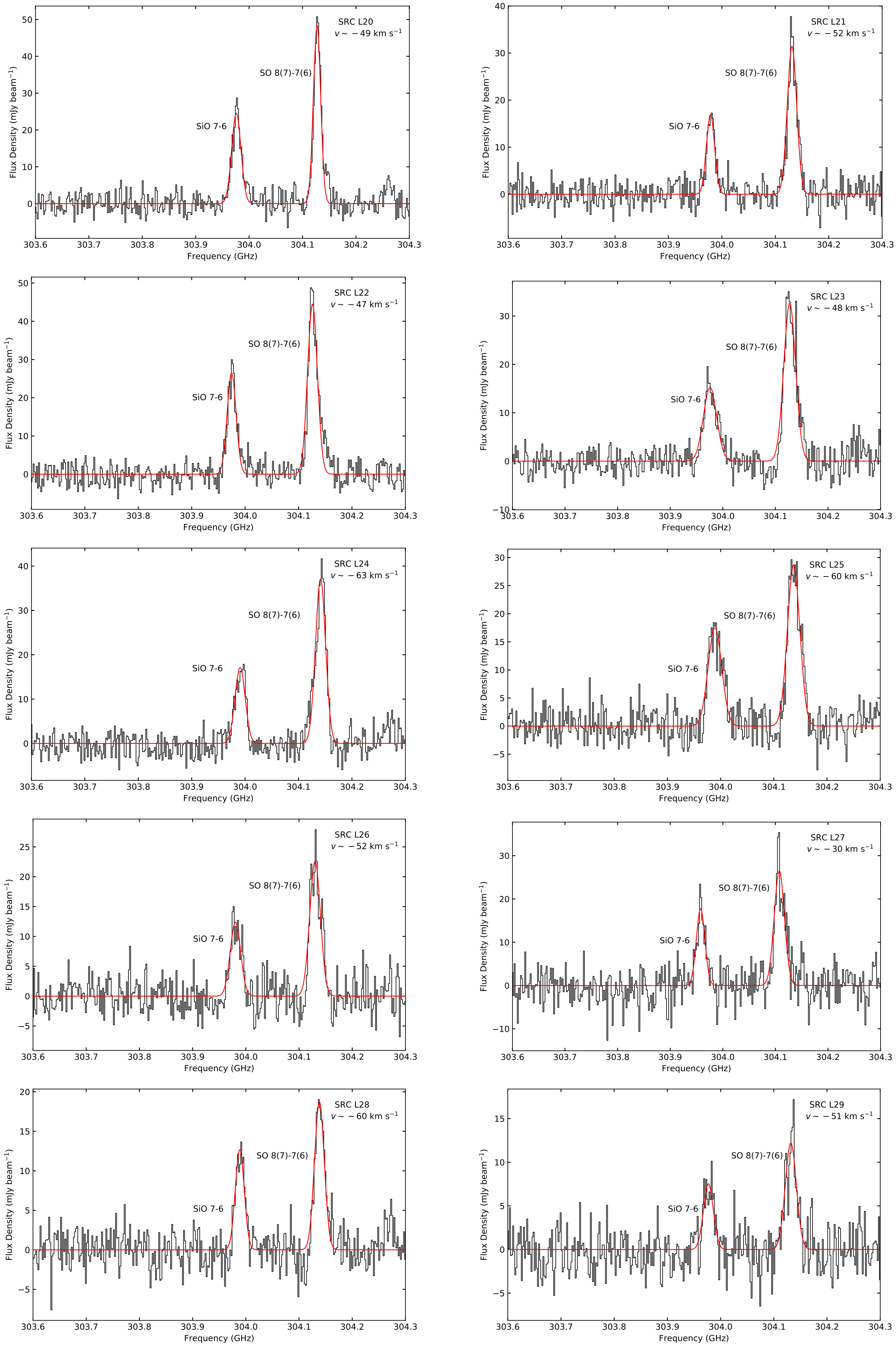
SRC L20
$v \sim -49$ km s^{-1}
SO 8(7)-7(6)
SiO 7-6
SRC L21
$v \sim -52$ km s^{-1}
SO 8(7)-7(6)
SiO 7-6
SRC L22
$v \sim -47$ km s^{-1}
SO 8(7)-7(6)
SiO 7-6
SRC L23
$v \sim -48$ km s^{-1}
SO 8(7)-7(6)
SiO 7-6
SRC L24
$v \sim -63$ km s^{-1}
SO 8(7)-7(6)
SiO 7-6
SRC L25
$v \sim -60$ km s^{-1}
SO 8(7)-7(6)
SiO 7-6
SRC L26
$v \sim -52$ km s^{-1}
SO 8(7)-7(6)
SiO 7-6
SRC L27
$v \sim -30$ km s^{-1}
SO 8(7)-7(6)
SiO 7-6
SRC L28
$v \sim -60$ km s^{-1}
SO 8(7)-7(6)
SiO 7-6
SRC L29
$v \sim -51$ km s^{-1}
SO 8(7)-7(6)
SiO 7-6
Flux Density (mJy beam^{-1})
Frequency (GHz)

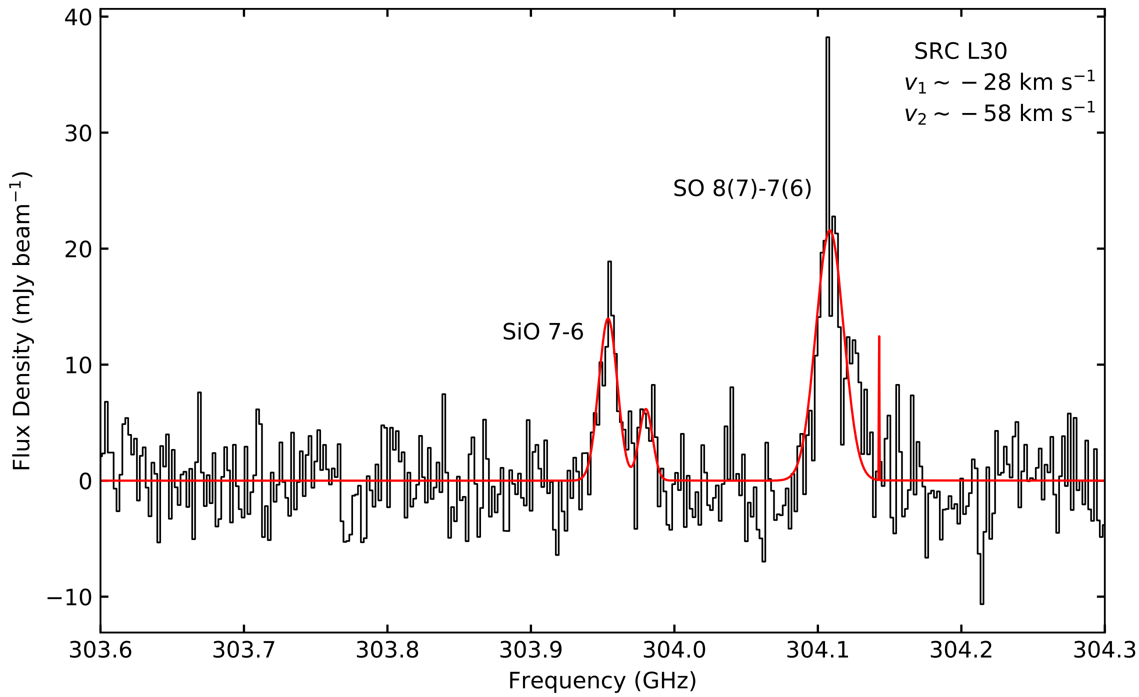
SRC L30
$v_1 \sim -28$ km s^{-1}
$v_2 \sim -58$ km s^{-1}
SO 8(7)-7(6)
SiO 7-6
Flux Density (mJy beam^{-1})
Frequency (GHz)

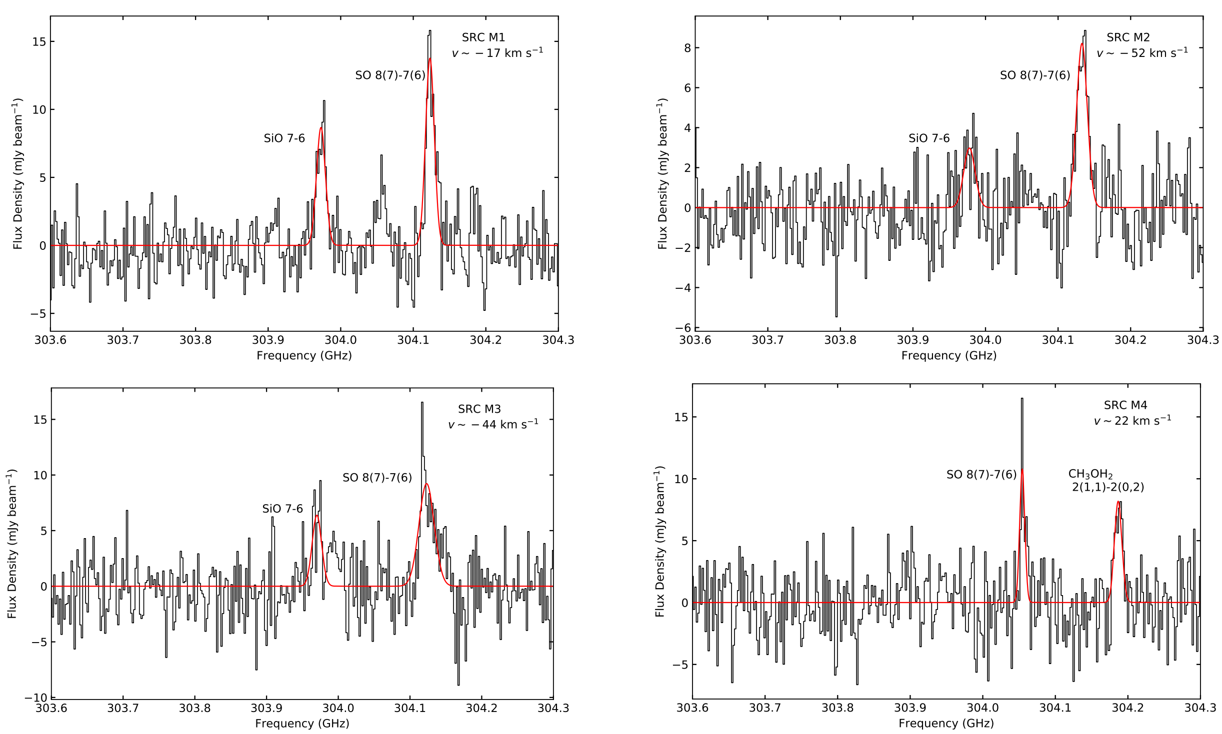
SRC M1
$v \sim -17$ km s^{-1}
SO 8(7)-7(6)
SiO 7-6
SRC M2
$v \sim -52$ km s^{-1}
SO 8(7)-7(6)
SiO 7-6
SRC M3
$v \sim -44$ km s^{-1}
SO 8(7)-7(6)
SiO 7-6
SRC M4
$v \sim 22$ km s^{-1}
SO 8(7)-7(6)
CH_3OH_2
2(1,1)-2(0,2)
Flux Density (mJy beam^{-1})
Frequency (GHz)

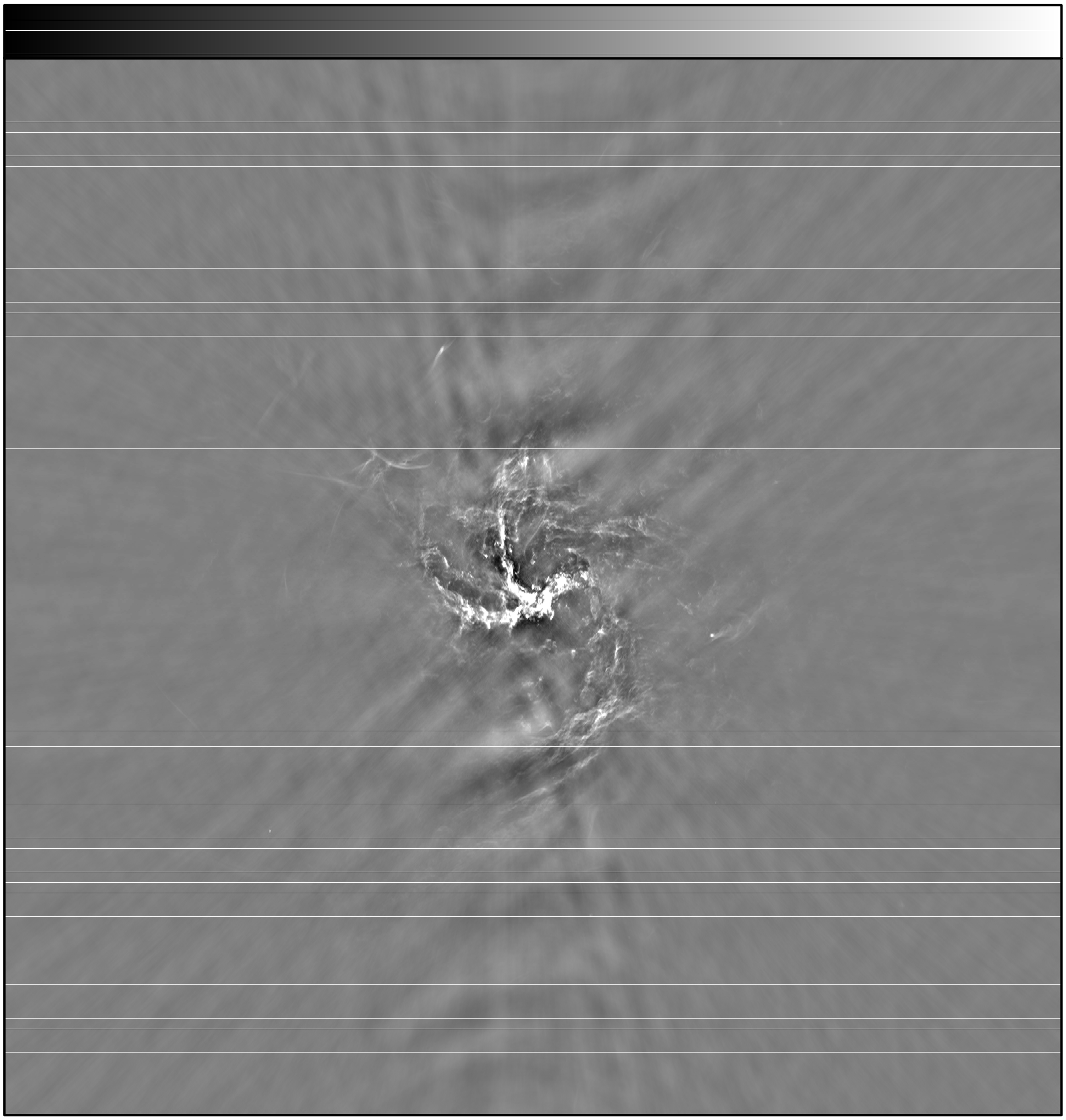

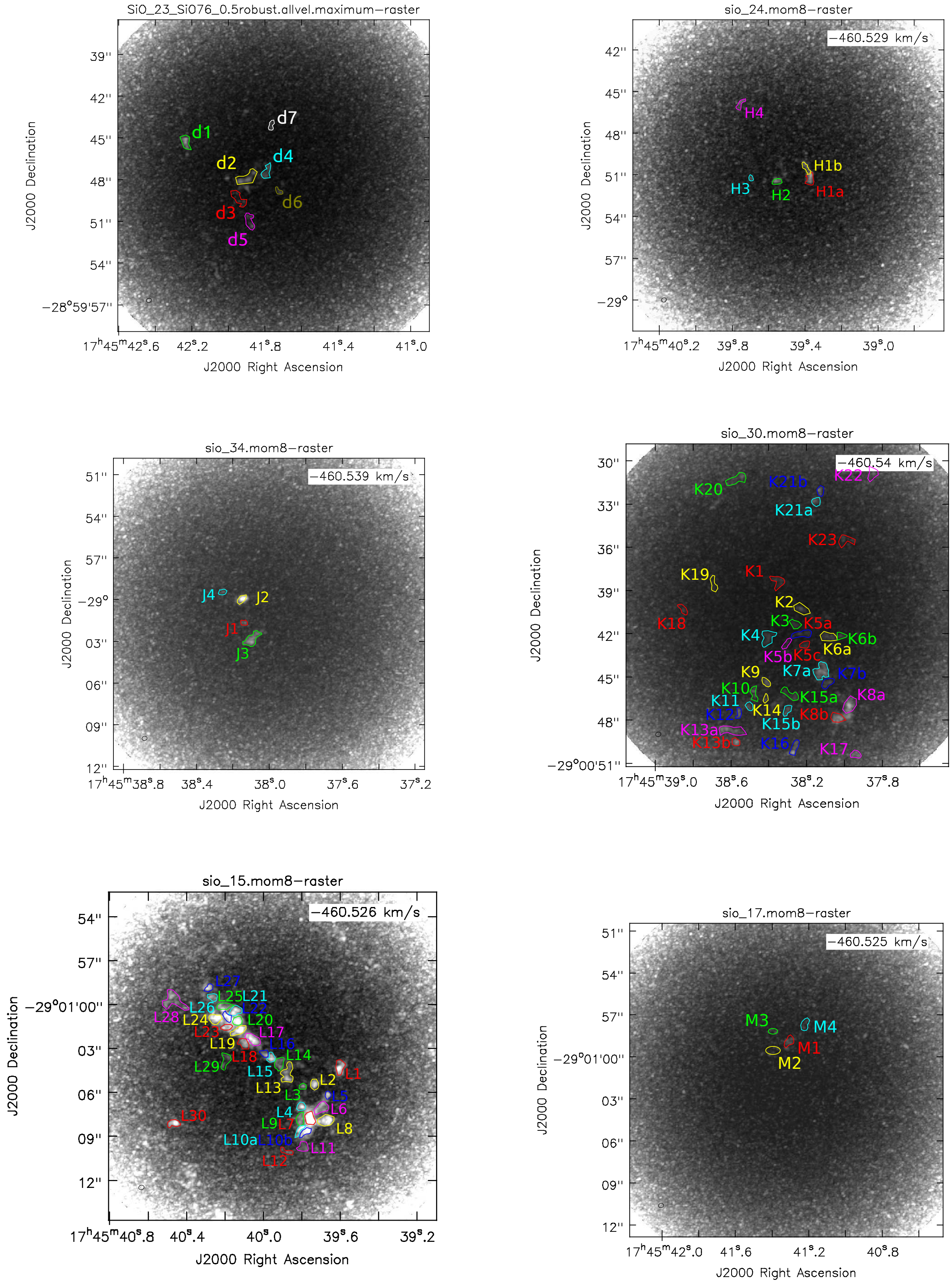

SiO_23_SiO76_0.5robust.allvel.maximum−raster
d1
d7
d2
d4
d6
d3
d5
J2000 Declination
J2000 Right Ascension
sio_24.mom8−raster
−460.529 km/s
H4
H1b
H3
H2
H1a
J2000 Declination
J2000 Right Ascension
sio_34.mom8−raster
−460.539 km/s
J4
J2
J1
J3
J2000 Declination
J2000 Right Ascension
sio_30.mom8−raster
−460.54 km/s
K20
K21b
K22
K21a
K23
K19
K1
K2
K18
K3
K5a
K4
K6b
K6a
K5b
K5c
K9
K7a
K7b
K10
K15a
K8a
K11
K12
K14
K8b
K15b
K13a
K13b
K16
K17
J2000 Declination
J2000 Right Ascension
sio_15.mom8−raster
−460.526 km/s
L27
L25
L21
L28
L26
L22
L24
L20
L23
L17
L19
L16
L18
L14
L29
L15
L1
L13
L2
L3
L5
L30
L4
L6
L9
L7
L8
L10a
L10b
L11
L12
J2000 Declination
J2000 Right Ascension
sio_17.mom8−raster
−460.525 km/s
M3
M4
M1
M2
J2000 Declination
J2000 Right Ascension